Dual-phase contrast-enhanced multislice computed tomography scans play a key role in the diagnosis of abdominal wall desmoid-type fibromatoses

Shengkai Li[a,1], Xiaodan Yuan[b,1], Zhijun Yi[c], Haiyang Dai[a], Lin Yang[d], Zhuozhi Dai[d] and Gen Yan[e,*]
[a]*Department of Radiology, Huizhou Central People's Hospital, Huizhou, Guangdong, China*
[b]*Department of Ultrasound, Huizhou Central People's Hospital, Huizhou, Guangdong, China*
[c]*Department of Pathology, Huizhou Central People's Hospital, Huizhou, Guangdong, China*
[d]*Department of Medical Imaging, The Second Affiliated Hospital, Medical College of Shantou University, Shantou, Guangdong, China*
[e]*Department of Radiology, The Second Affiliated Hospital of Xiamen Medical College, Xiamen, Fujian, China*

Abstract.
BACKGROUND: Abdominal wall desmoid-type fibromatoses (AWDF) are occasionally encountered in clinical work, but related CT reports are rare, and most cases were misdiagnosed as malignant tumors.
OBJECTIVE: We aimed to determine the diagnostic value of multislice computed tomography (MSCT) in relation to the clinical diagnosis of AWDF.
METHODS: The medical records of 14 patients whose pathology results provided initial confirmation of AWDF were reviewed, and data describing their clinical characteristics, tumors' MSCT characteristics, and the condition of the surrounding tissues were analyzed and summarized retrospectively. Intraobserver and interobserver reproducibilities were evaluated.
RESULTS: AWDF tended to occur in women of childbearing age (24–32 years). They occurred more frequently during the first year following pregnancy. The mean disease duration was 5.64 ± 3.78 months. All isolated tumors were growing along the musculoaponeurotic layer, and their maximum diameters were between 32 and 76 mm. Tumors' capsules were incomplete, and although the tumors infiltrated the surrounding muscles, the surrounding fat tissue and vessels were not infiltrated. None of the patients' tumors showed cystic degeneration, calcification, necrosis, or peritumoral edema. The tumors had slightly lower densities on the pre-contrast enhancement scans and mild-to-moderate enhancement after contrast enhancement. All tumors contained ribbon-like structures, and approximately 65% of the tumors encircled vascular structures.
CONCLUSION: Dual-phase contrast-enhanced MSCT scans were associated with a high level of diagnostic efficacy for AWDF. The abdominal wall masses grew along the musculoaponeurotic layer, which, together with the ribbon-like structures within the tumors, should prompt clinicians to consider the presence of AWDF.

Keywords: Abdominal, desmoid-type fibromatoses, computed tomography, diagnosis

---

[1]These authors contributed equally to the work and should be considered co-first authors.
*Corresponding author: Gen Yan, Department of Radiology, The Second Affiliated Hospital of Xiamen Medical College, Xiamen, Fujian, China. E-mail: gyan@stu.edu.cn.

1. Introduction

Desmoid-type fibromatoses (DF), which are also known as aggressive or musculoaponeurotic fibromatoses, are rare, histopathologically benign fibroblastic tumors that are found in the musculoaponeurotic system [1]. The annual incidence of DF is 2.4–4.3 cases per million inhabitants in European countries [2]. DF can develop at almost any body site, but they tend to develop in the abdominal wall and soft tissues of the extremities, shoulder, neck, and chest wall [3]. DF never metastasize, but they are notorious for their infiltrative growth and local recurrence [4]. With the exception of a limited number of radiologic case reports, previous reports that describe DF have focused mostly on their clinical and pathologic features and treatment [5–7]. Although some radiologic reports describe DF, most do not specify their locations, or they only provide ambiguous descriptions of the tumors' imaging characteristics that could be useful for diagnosing and differentiating DF from other masses [8,9].

Ultrasound is the first-line imaging technique for palpable lumps, but it is non-specific. Although the resolution of magnetic resonance imaging (MRI) is good for soft tissue tumors, it is readily affected by abdominal wall motion artifacts, and it cannot easily be performed in community hospitals that have limited resources. Multislice computed tomography (MSCT) is an inexpensive and widely available imaging tool that is useful for evaluating abdominal wall masses in particular clinical settings. Therefore, we retrospectively evaluated 14 patients with pathology-confirmed abdominal wall DF (AWDF) at our hospital to determine whether MSCT can generate useful diagnostic information about AWDF.

2. Patients and methods

2.1. Patient selection

We searched the pathology and radiology databases at our institution and identified 21 patients who had pathology-confirmed AWDF from January 2013 to January 2020. Of the 21 patients, six patients' preoperative radiologic images were not available, and one patient had a tumor recurrence; these patients were excluded. Hence, 14 patients with a mean age of 29 (range, 24–32) years were enrolled to participate in this study. The enrolled patients' clinical records were thoroughly reviewed regarding data describing their medical histories, clinical presentations, and physical examinations. This retrospective study was conducted with the consent of the Medical Ethics Committee.

2.2. Multislice computed tomography

All patients underwent pre-contrast-enhanced and contrast-enhanced MSCT scans using a 128MSCT scanner (Lightspeed; GE Healthcare), and all aspects of the lesions were scanned within the entire abdomen or hypogastrium using the following parameters: tube voltage: 120 kV, tube current: 400–500 mA, acquisition layer thickness: 0.625 mm, rotation time: 1.0 s, reconstruction layer thickness and interval: 5 mm, and pitch: 0.99. For contrast enhancement, ioversol (75 mL at 350 mg/mL) was injected into the forearm at a speed of 2.5–3.0 mL/s using a high-pressure syringe (Nemoto Kyorindo Co., Ltd.), and dual-phase contrast-enhanced MSCT was performed for 30 s in the arterial phase and 60 s in the venous phase.

2.3. Image analysis

Initially, all images were analyzed independently by two senior radiological diagnosticians (SL and

GY) who were blinded to the patients' pathological findings and who had 8 years and 15 years of clinical experience of diagnosing disease from CT images. Consensus was sought regarding (1) a tumor's size, shape, boundaries, calcification, necrosis, cystic degeneration, and enhancement pattern; (2) the conditions surrounding a tumor, including peritumoral edema, and changes to and invasion of the surrounding vessels, fat, and muscles; and (3) the condition of the abdominal cavity, including the presence of seroperitoneum and lymphatic metastasis. Two weeks later, the two radiologists reinterpreted the scans. A tumor's diameter was measured in the long axis, and its shape was determined according to whether the lesion was elongated along the musculoaponeurotic plane. The intensities of the lesions on the MSCT scans were compared qualitatively with those of the adjacent normal muscles where the lesion was most dominant. The degrees of enhancement were assessed subjectively as none, mild, moderate, and distinct. The presence of unenhanced bands with low signal intensities was identified if there were structures that showed low-density areas without enhancement. Disagreements were resolved by consultation.

2.4. Pathological analysis

All 14 patients underwent surgical resections. The pathological specimens were fixed with 4% formaldehyde, and tissue sections underwent hematoxylin and eosin and immunohistochemical staining. All of the tissue sections were reviewed by the same senior pathologist. The AWDF diagnostic criteria included the proliferation of elongated, slender, spindle-shaped cells of uniform appearance with variable cellularity, infrequent mitoses and atypia, and frequently occurring and poorly defined fascicles in the collagenous stroma.

2.5. Statistical analysis

Interobserver and intraobserver agreements were determined by calculating simple kappa values for subjective parameters. Kappa values < 0.20 indicated poor agreement, 0.21–0.40 fair agreement, 0.41–0.60 moderate agreement, 0.61–0.80 good agreement, and > 0.81 excellent agreement.

3. Results

Table 1 summarizes the clinical and MSCT characteristics of the 14 patients with AWDF. All patients enrolled in this study were female who had no family history of AWDF. The patients' mean age was 28.6 ± 2.2 (range, 24–32 years) years, and the mean disease duration was 5.6 ± 3.7 months. Six patients (42.8%) had a history of surgery, and six patients (42.8%) were aware of a dull pain. Physical examinations showed that the patients' abdominal walls were raised locally, the skin temperature was not high, and redness, swelling, and ulceration were not evident on the surface. Palpation revealed that the masses were hard and their ranges of motion were poor, and they had little effect on breathing and posture. There were no vascular murmurs during auscultation. The laboratory test results showed that the C-reactive protein, alpha-fetoprotein, carcinoembryonic antigen, and ferritin levels were within the normal ranges.

3.1. Imaging characteristics of abdominal wall desmoid-type fibromatoses

The intraobserver and interobserver agreements for the subjective MSCT features were excellent (Table 2). All 14 patients had solitary lateral masses in the anterior abdominal wall. Most of the tumors

Table 1
Clinical and multislice computed tomography characteristics in 14 patients with AWDF

Patient no./sex/age, years	Pain	History of surgery	Laboratory results			Location	Size, mm	Shape	Unenhanced/enhanced/delay CT value, HU	MSCT features						
			CEA	AFP	CRP					Normal vessels	Muscle thickening	Fat invasion	Cystic degeneration	Necrosis	Calcification	Edema
1/F/30	−	−	−	−	−	OEA	36	Lobulated	33/61/76	+	+	−	−	−	−	−
2/F/32	−	+	−	−	−	UC	71	Oval	28/31/42	−	−	−	−	−	−	−
3/F/26	+	−	−	−	−	OEA	45	Oval	30/39/48	+	+	−	−	−	−	−
4/F/24	−	−	−	−	−	OEA	76	Oval	24/34/47	−	−	−	−	−	−	−
5/F/31	+	+	−	−	−	OIA	58	Oval	36/62/72	+	−	−	−	−	−	−
6/F/29	+	−	−	−	−	OIA	62	Lobulated	28/42/48	−	+	−	−	−	−	−
7/F/29	+	−	−	−	−	UC	32	Oval	40/68/74	+	−	−	−	−	−	−
8/F/30	+	+	−	−	−	UC	57	Oval	32/43/48	+	+	−	−	−	−	−
9/F/32	−	+	−	−	−	OEA	59	Lobulated	31/48/53	+	−	−	−	−	−	−
10/F/29	−	−	−	−	−	UC	42	Oval	41/68/85	+	+	−	−	−	−	−
11/F/32	−	+	−	−	−	OEA	48	Lobulated	36/54/69	−	+	−	−	−	−	−
12/F/25	−	−	−	−	−	UC	64	Oval	32/44/53	+	+	−	−	−	−	−
13/F/26	+	−	−	−	−	OEA	41	Lobulated	40/65/83	−	+	−	−	−	−	−
14/F/29	−	+	−	−	−	OEA	32	Lobulated	28/43/52	+	−	−	−	−	−	−

AFP, alpha-fetoprotein; CEA, carcinoembryonic antigen; CRP, C-reactive protein; CT, computed tomography, F, female; MSCT, multislice computed tomography; OEA, obliquus externus abdominis; OIA, obliquus internus abdominis, UC, unclear.

Table 2
Intraobserver and interobserver agreements for the subjective multislice computed tomography characteristics

MSCT characteristic	Kappa value for intraobserver agreement (agreement number/total)		Kappa value for interobserver agreement (agreement number/total)
	Observer 1	Observer 2	
Shape	1	1	1
Size	0.950	1	0.899
Enhancement pattern	0.965	1	0.955
Vessel invasion	0.969	0.910	0.879
Muscle invasion	1	0.943	0.925
Fat invasion	1	1	1
Cystic degeneration	1	1	1
Necrosis	1	1	1
Calcification	1	1	1
Edema	0.987	1	0.912

MSCT, multislice computed tomography.
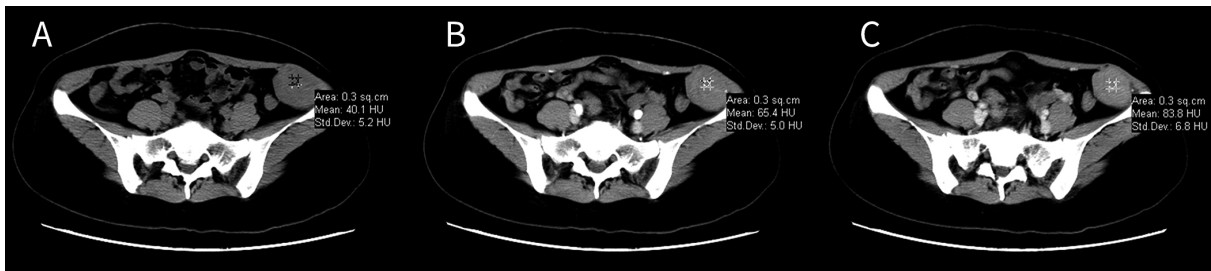
Fig. 1. Images from the same patient with an abdominal wall desmoid-type fibromatosis. A) Pre-contrast-enhanced computed tomography image showing a mixed, slightly low-density tumor without cystic degeneration, calcification, or necrosis. B) Arterial phase image with mild-to-moderate contrast enhancement. C) Venous phase image with further enhancement.

were located in the abdominal oblique muscle, grew along the long axis of the musculoaponeurotic layer, and were oval or shallowly lobulated, and the tumors' largest dimensions ranged from 32 mm to 76 mm (mean, 51.6 mm). The pre-contrast-enhanced CT images showed that compared with the surrounding muscles, the tumors had slightly lower densities (Fig. 1A) and a mean CT value of 32.8 ± 4.2 HU. Most of the masses demonstrated mild-to-moderate enhancement in the arterial phase (Fig. 1B), and the mean CT value was enhanced by 17.3 ± 6.8 HU. The venous phase further enhanced the masses (Fig. 1C), and the mean CT value reached 60.7 ± 13.5 HU. The vessels within the abdominal wall around the tumor were normal, and in nine patients, some branches of the vessels entered the tumors without being destroyed (Fig. 2). Typically, the tumors occurred intermuscularly, were located along the musculoaponeurotic layer, and did not invade the surrounding fat tissue (Figs 2 and 3A and B). The surrounding infiltrated muscles had thickened to create a "torch-like" appearance in eight patients (Fig. 3C). None of the patients' tumors showed cystic degeneration, necrosis, or calcification, and peritumoral edema, invasion of the surrounding fat tissue, peritoneal effusion, destruction of adjacent bone, and lymph node metastasis were not evident in any of the patients. Notably, all patients had slightly high densities of ribbon-like structures within their tumors; these ribbon-like structures were clearly enhanced on the contrast-enhanced scans (Figs 1–3).

3.2. Pathologic features of abdominal wall desmoid-type fibromatoses

The pathologic examinations showed that the masses were firm, and that the capsules were incomplete
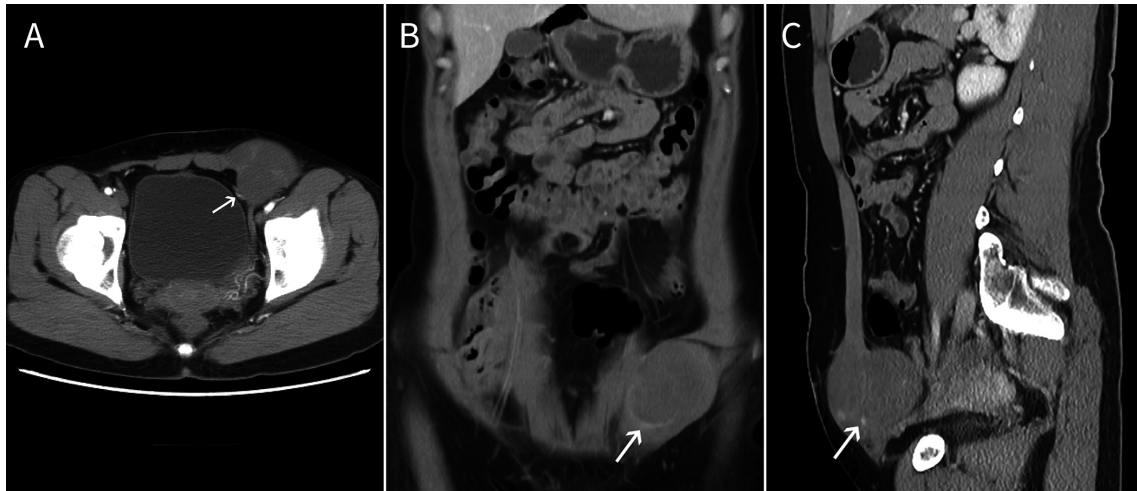
Fig. 2. A) A shallowly lobulated mass. B) and C) Computed tomography reconstruction shows the mass was invading and growing along the internal oblique abdominal muscle without invading the surrounding fat tissue. The arrows show that the surrounding vessel was preserved while the surrounding muscle was invaded and became bulky.
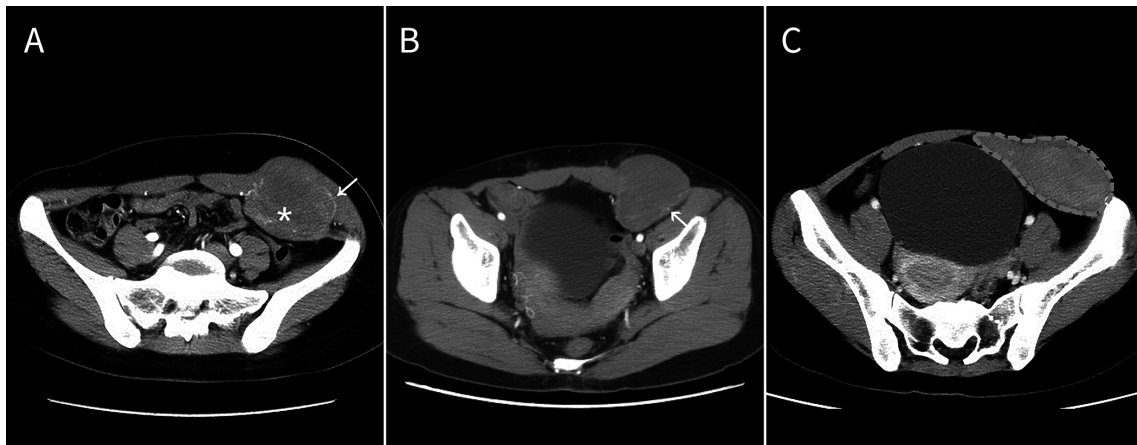
Fig. 3. A) A ribbon-like enhanced structure (asterisk) was seen within the tumor, and the normal blood vessels of the abdominal wall surrounded the tumor and they partially entered the tumor (arrow). The mass infiltrated the rectus abdominis muscle and thickened the invaded muscle to form (C) a "torch-like" structure with the mass.

(Fig. 4A). When sliced, the specimens were grayish white or grayish red with woven textures (Fig. 4B). Histologically, the tumors comprised different proportions of spindle cells, namely, fibroblasts and myofibroblasts, collagen fibers, and mucous matrix. The spindle cells were interlaced or swirled and were surrounded by collagen and mucus. The cell staining was uniform, and atypia, cystic degeneration, necrosis, and calcified particles were not evident (Fig. 4C). The immunocytochemical analysis showed that the tumor cells were positive for β-catenin and vimentin, and $< 10\%$ were positive for *Ki67* (Fig. 4D–F).

4. Discussion

The 2013 World Health Organization classification categorizes DF as borderline soft tissue tumors [10].
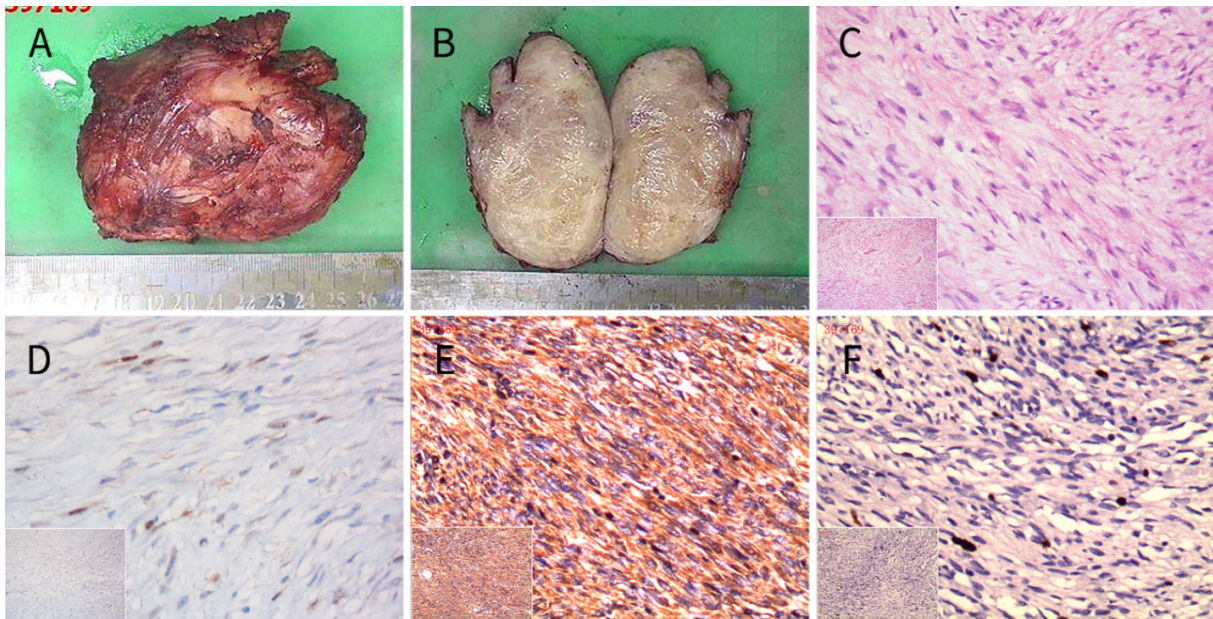
Fig. 4. A) A tumor with a partially incomplete capsule. B) The cut tumor was grayish-white and had a braided texture and no obvious liquefaction or necrosis. C) Under a light microscope, the spindle cells were woven or swirled, and cell atypia was not obvious (hematoxylin and eosin × 100). Immunocytochemically, D) the tumor cells were positive for β-catenin, E) the tumor cells were positive for vimentin, and F) < 10% of the cells were positive for *Ki67*.

Although DF never metastasize, they are invasive and often recur postoperatively [11]. The etiology of DF remains unclear, and they are hypothesized to be caused by multiple factors, including trauma, surgery, pregnancy, hormones, and genetics [12].

All 14 patients in this study were aged between 20 and 30 years; hence, they were young women of childbearing age. Two patients' AWDF occurred during their first pregnancies, and 12 patients' AWDF occurred during or after their second pregnancies. The high incidence of AWDF in the women during pregnancy, which is consistent with previous studies' findings [13,14], indicates that estrogens may be involved in the development and evolution of the disease. The findings from preclinical studies of DF development in pigs after the prolonged administration of estrogens support this hormonal dependency, and several studies' findings have demonstrated estrogen receptor positivity in up to 90% of neoplasms [15, 16].

DF can occur at sites of previous surgery or blunt trauma [17]. We rarely find AWDF in patients who undergo appendectomy, abdominal hernia repair, and other abdominal wall surgeries, despite these procedures causing similar levels of trauma to the abdominal wall muscles as a cesarean delivery. We hypothesize that AWDF might be caused by the increases in abdominal pressure that occur during late gestation that result in some fibroblast and myofibroblast mutations during repeated injury and repair processes over a prolonged period. Therefore, we consider that abdominal surgery may not cause tumorigenesis directly, but it may increase the fragility of the natural barrier provided by the abdominal wall, and that this weakness may render it more prone to pathological changes when it is exposed to factors that cause long-term chronic injuries, including high abdominal pressure during pregnancy.

Ultrasound is the most common method used to evaluate a surface mass mainly because of it has the advantages of non-invasive, low cost, simple operation, good medical compliance. However, there are few reports on the ultrasonic diagnosis of AWDF at present. Most of they were only get some preliminary

diagnostic information by judging whether the mass was from muscle tissue, determining the cystic solid of the mass and measuring the size of the mass, which cannot make a good qualitative diagnosis [18,19]. Although ultrasonography is the first method used to evaluate a surface mass, it lacks specificity and has a high misdiagnosis rate. MRI offers multidirectional imaging of soft tissue, and its resolution is high, but limitations associated with respiratory artifacts and the availability of MRI equipment have caused difficulties in relation to its widespread use in community hospitals. MSCT is associated with good temporal and spatial resolution, and CT examinations are common in community hospitals. A summary of the features of MSCT that may play a role in the diagnosis of AWDF follows, which is based on information from previously published sporadic reports and our findings. First, isolated intramuscular masses with slightly lower mixed densities and without cystic degeneration, calcification, necrosis, or peritumoral edema should prompt clinicians to consider AWDF. All patients in the current study had isolated masses within the anterior abdominal wall muscles, and the masses were most commonly found in the internal oblique muscle (12 patients). The masses were elliptical or lobulated, and cystic degeneration, necrosis, calcification, and evident peritumoral edema were not found in any of the patients, which concurs with previous studies' findings [20,21]. Second, evaluations using a soft tissue window during pre-contrast-enhanced CT scans revealed slightly higher density ribbon-like structures within the masses that were visibly enhanced during the contrast-enhanced CT scans. These findings were observed in all of the patients in this study. Taking these findings together with those reported previously [21,22], we believe that this sign is caused by different ratios of fibrous tissue, collagen, and mucus within the tumor. The areas of dense fibrous tissue form the ribbon-like structures with a slightly higher density, whereas the areas of mucus and collagen form a low-intensity background. Therefore, we believe that the "ribbon sign" is a characteristic feature of AWDF on CT images. Third, the tumors invade the surrounding muscle tissue but not the fat tissue, and they can encase vessels without destroying vascular plexuses. Of the 14 patients, 11 showed signs of tumor invasion into the adjacent muscles, but abdominal wall fat infiltration and peripheral vascular plexus destruction were not found in any of the patients. The capsules of fibromas are often incomplete, and finger-like extensions from the tumors, which are similar to tentacles, interweave with the adjacent normal muscle fibers [9,23]. This may explain the local invasion characteristics of these tumors. As there are no muscle fibers in the fat layer of the abdominal wall, the tumor cells cannot interweave with the fat cells; hence, AWDF invade muscle tissue but not fat tissue. Therefore, the peripheral vascular plexuses are preserved, and the capillary networks can be observed inside the tumors. These findings are consistent with the benign cytological and malignant biological characteristics of AWDF, and we believe that they have important implications for the diagnosis of AWDF using MSCT.

AWDF are relatively rare; consequently, doctors have limited knowledge about and experience of AWDF, and their diagnostic skills are insufficient. The failure to identify the atypical MSCT signs of AWDF led to a significantly high clinical misdiagnosis rate. Differentiating between soft tissue sarcomas, endometriosis, solitary fibrous tumors, and AWDF is important. Compared with AWDF, soft tissue sarcomas progress faster, pain emerges earlier and is more intense, and liquefied, necrotic areas and focal calcification are often observed within these tumors, and disruption of structures adjacent to these tumors is more visible on CT scans [24]. Among the patients in this study, five complained of focal enlargement and tenderness that were evident for a few months before admission, and these signs, coupled with the hard texture and poor mobility of a mass, may lead to clinical misdiagnoses of soft tissue sarcomas. However, MSCT can distinguish between AWDF and soft tissue sarcomas. For example, the interiors of AWDF are composed of different proportions of fibrous tissue and collagen, and CT revealed slightly low-density and ribbon-like structures rather than the disorganized areas of liquefaction and necrosis

that characterize sarcomas. Furthermore, compared with soft tissue sarcomas, the density of AWDF is lower and their degree of enhancement is less evident. When these characteristics are considered in conjunction with calcification and infiltration, distinguishing between AWDF and soft tissue sarcomas becomes more straightforward. Since AWDF often occur in young women and some patients have a history of surgery, patients may be diagnosed with endometriosis rather than AWDF. However, AWDF are not associated with menstrual pain or menstrual enlargement. In addition, the shape of endometrial tissue is more irregular, its density is higher with a CT value similar to that of muscle, and the degree of enhancement is more evident [25]. Solitary fibrous tumors are benign mesenchymal tissue-derived masses with intact capsules that rarely invade the surrounding tissue. Distinguishing between solitary fibrous tumors and AWDF is not difficult, because the former is characterized by lobulated masses and significant total tumor enhancement [26].

In addition to the intrinsic limitations of the retrospective nature of the study, this study had a small sample size because AWDF are rare. However, to the best of our knowledge, this is the largest analysis of the clinical and imaging characteristics of AWDF to date, and this study's findings show that AWDF have particular clinical manifestations and imaging characteristics. Consequently, if a single abdominal wall mass is encountered in women of childbearing age, clinicians can be more confident regarding the differential diagnosis of AWDF if they combine the clinical information with the aforementioned imaging features.

5. Conclusion

AWDF had prominent clinical, histopathological, and radiological features. Dual-phase contrast-enhanced MSCT scans were associated with a high level of diagnostic efficacy for AWDF. The differential diagnosis from other tumors was obtained by thorough analysis and comparison of the similar and different characteristics.

Acknowledgments

Conflict of interest

None to report.

References

[1] De Schepper AM, Vandevenne JE. Tumors of fibrous tissue. In: De Schepper AM, Parizel PM, De Beuckeleer L, eds. Imaging of soft tissue tumors. Berlin Heidelberg New York: Springer. 2001.

[2] Penel N, Coindre JM, Bonvalot S, Italiano A, Neuville A, Le Cesne A, et al. Management of desmoid tumours: A nationwide survey of labelled reference centre networks in France. Eur J Cancer. 2016; 58: 90-96.

[3] Jo VY, Fletcher CD. WHO classification of soft tissue tumours: An update based on the 2013 (4th) edition. Pathology. 2014; 46: 95-104.

[4]   Dinauer PA, Brixey CJ, Moncur JT, Fanburg-Smith JC, Murphey MD. Pathologic and MR imaging features of benign fibrous soft-tissue tumors in adults. Radiographics. 2007; 27: 173-187.

[5]   Escobar C, Munker R, Thomas JO, Li BD, Burton GV. Update on desmoid tumors. Ann Oncol. 2012; 23: 562-569.

[6]   Gounder MM, Mahoney MR, Van Tine BA, Ravi V, Attia S, Deshpande HA, et al. Sorafenib for advanced and refractory desmoid tumors. N Engl J Med. 2018; 379: 2417-2428.

[7]   Kasper B, Baumgarten C, Garcia J, Bonvalot S, Haas R, Haller F, et al. An update on the management of sporadic desmoid-type fibromatosis: A European Consensus Initiative between Sarcoma PAtients EuroNet (SPAEN) and European Organization for Research and Treatment of Cancer (EORTC)/Soft Tissue and Bone Sarcoma Group (STBSG). Ann Oncol. 2017; 28: 2399-2408.

[8]   Eastley N, McCulloch T, Esler C, Hennig I, Fairbairn J, Gronchi A, et al. Extra-abdominal desmoid fibromatosis: A review of management, current guidance and unanswered questions. Eur J Surg Oncol. 2016; 42: 1071-1083.

[9]   Braschi-Amirfarzan M, Keraliya AR, Krajewski KM, Tirumani SH, Shinagare AB, Hornick JL, et al. Role of imaging in management of desmoid-type fibromatosis: A primer for radiologists. Radiographics. 2016; 36: 767-782.

[10] Fletcher CDM, Bridge JA, Hogendoorn PCW, Mertens F. WHO classification of tumours of soft tissue and bone, 4th edn. Lyon: IARC Press. 2013; 110-111.

[11] Skubitz KM. Biology and treatment of aggressive fibromatosis or desmoid tumor. Mayo Clin Proc. 2017; 92: 947-964.

[12] Okuno S. The enigma of desmoid tumors. Curr Treat Options Oncol. 2006; 7: 438-443.

[13] Penel N, Chibon F, Salas S. Adult desmoid tumors: Biology, management and ongoing trials. Curr Opin Oncol. 2017; 29: 268-274.

[14] Fiore M, Coppola S, Cannell AJ, Colombo C, Bertagnolli MM, George S, et al. Desmoid-type fibromatosis and pregnancy: A multi-institutional analysis of recurrence and obstetric risk. Ann Surg. 2014; 259: 973-978.

[15] Janinis J, Patriki M, Vini L, Aravantinos G, Whelan JS. The pharmacological treatment of aggressive fibromatosis: A systematic review. Ann Oncol. 2003; 14: 181-190.

[16] Deyrup AT, Tretiakova M, Montag AG. Estrogen receptor-beta expression in extraabdominal fibromatoses: An analysis of 40 cases. Cancer. 2006; 106: 208-213.

[17] Nakayama T, Tsuboyama T, Toguchida J, Hosaka T, Nakamura T. Natural course of desmoid-type fibromatosis. J Orthop Sci. 2008; 13: 51-55.

[18] Xu W, Lv K, Huang Y, Wen Q, Pan M, Huang P. Features of ultrasound and contrast enhanced ultrasound in superficial desmoid-type fibromatosis: A series of 19 cases. Clin. Hemorheol Microcirc.

[19] Milos RI, Moritz T, Bernathova M, et al. Superficial desmoid tumors: MRI and ultrasound imaging characteristics. Eur J Radiol. 2015; 84(11): 2194-2201.

[20] Walker EA, Petscavage JM, Brian PL, Logie CI, Montini KM, Murphey MD. Imaging features of superficial and deep fibromatoses in the adult population. Sarcoma. 2012; 2012: 215810.

[21] Dinauer PA, Brixey CJ, Moncur JT, Fanburg-Smith JC, Murphey MD. Pathologic and MR imaging features of benign fibrous soft-tissue tumors in adults. Radiographics. 2007; 27: 173-187.

[22] Garcia-Ortega DY, Martín-Tellez KS, Cuellar-Hubbe M, Martínez-Said H, Álvarez-Cano A, Brener-Chaoul M, et al. Desmoid-type fibromatosis. Cancers (Basel). 2020; 12: 1851.

[23] Martínez Trufero J, Pajares Bernad I, Torres Ramón I, Hernando Cubero J, Pazo Cid R. Desmoid-type fibromatosis: Who, when, and how to treat. Curr Treat Options Oncol. 2017; 18: 29.

[24] Levy AD, Manning MA, Al-Refaie WB, Miettinen MM. Soft-tissue sarcomas of the abdomen and pelvis: Radiologic-pathologic features, part 1-common sarcomas: From the radiologic pathology archives. Radiographics. 2017; 37: 462-483.

[25] Leone Roberti Maggiore U, Ferrero S, Mangili G, Bergamini A, Inversetti A, Giorgione V, et al. A systematic review on endometriosis during pregnancy: Diagnosis, misdiagnosis, complications and outcomes. Hum Reprod Update. 2016; 22: 70-103.

[26] Demicco EG, Park MS, Araujo DM, Fox PS, Bassett RL, Pollock RE, et al. Solitary fibrous tumor: A clinicopathological study of 110 cases and proposed risk assessment model. Mod Pathol. 2012; 25: 1298-1306.